Theory of photoluminescence from modulation-doped self-assembled quantum dots in a magnetic field
Wojs, Arkadiusz; Hawrylak, Pawel

National Research Council Canada   Conseil national de recherches Canada

Canada

Theory of photoluminescence from modulation-doped self-assembled quantum dots in a magnetic field

Arkadiusz Wojs* and Pawel Hawrylak

Institute for Microstructural Sciences, National Research Council of Canada, Ottawa, Canada K1A 0R6

(Received 1 November 1996)

We study the effect of free carriers on photoluminescence from modulation-doped self-assembled quantum dots. Exact diagonalization studies of up to $N=8$ electrons and a single exciton in InAs self-assembled dots, and a Hartree-Fock calculations for up to $N=20$ electrons, are carried out. The total spin and total angular momentum are found to oscillate with the number of electrons. The photoluminescence spectrum is calculated and the band-gap renormalization in zero-dimensional systems is discussed. The tendency of electrons in degenerate, partially filled electronic shells to maximize the total spin leads to a strong dependence of the spectrum on the number of electrons N, the magnetic field B, and the polarization of light. [S0163-1829(97)04320-8]

I. INTRODUCTION

An epitaxial growth of strained InAs layers on GaAs is unstable and leads to a spontaneous formation of InAs-rich quasi-two-dimensional islands.[1] The shape, and hence the electronic properties, of these self-assembled quantum dots (SAD's) depend on growth conditions.[1-9] SAD's in the shape of pyramids,[2,3] disks,[4] and lenses[1,5-8] have been reported. We study here a class of lens-shaped InAs SAD's, investigated recently by the single electron capacitance,[6,8,10] far-infrared (FIR),[6,10] and photoluminescence (PL) spectroscopies.[1,6-8,11] In the capacitor structures[6,8,10] an external gate and a modulation-doped back layer allowed for charging of SAD's with electrons. The changes in capacitance monitored the number of electrons N. The FIR spectroscopy measured internal transitions of few-electron complexes in SAD's.[10,11] The FIR transitions were a fingerprint of the electronic structure of N electrons in the dot. The electronic structure was shown[11] to depend strongly on the occupation of electronic shells, with an oscillatory behavior of the total spin and the total angular momentum in accordance with Hund's rule. A combination of high-intensity PL of undoped SAD's and capacitance spectroscopy[8] allowed for the determination of the valence-hole energy spectrum. The combination of capacitance, photoluminescence, and high-intensity photoluminescence verified a basic picture of shells[12] of electron and valence-hole states in lens-shaped SAD's.

It is interesting to ask at this stage how the photoluminescence from modulation-doped SAD's can be used directly to understand the correlated electronic states in 0D systems. There has been already preliminary theoretical work on the optical properties of correlated electrons in quantum dots with small confinement in a strong magnetic field.[13-15] Here we concentrate on the experimentally available system of InAs self-assembled dots. Using exact diagonalization techniques we investigate the effects of electron-electron and electron-valence hole interactions on the photoluminescence spectrum of an InAS SAD charged with many electrons. We show that the PL spectrum measures the spectral function of

a hole in the correlated electronic state of the SAD. Because, in agreement with Hund's rules, a partially filled electronic shell acquires a maximum total spin, the PL turns out to be a sensitive function of the number of electrons N, the magnetic field B, and the polarization of light.

II. THE MODEL

We study the interband recombination of a single electron valence-hole pair, confined in a modulation-doped self-assembled quantum dot. The electron valence-hole pair interacts with additional $N-1$ electrons. To describe the initial state we consider a system of N electrons and a single valence-band hole, confined in a quantum dot and interacting via Coulomb forces.[13-15] The final state corresponds to a system of $N-1$ electrons and a photon. Using composite indices i to describe single-particle states $|i\rangle$, the initial-state many-particle Hamiltonian can be written as

$$H = \sum_i \varepsilon_i^e c_i^\dagger c_i + \sum_i \varepsilon_i^h h_i^\dagger h_i + \frac{1}{2} \sum_{ijkl} \langle ij|V_{ee}|kl\rangle c_i^\dagger c_j^\dagger c_k c_l$$

$$+ \sum_{ijkl} \langle ij|V_{eh}|kl\rangle c_i^\dagger h_j^\dagger h_k c_l. \qquad (1)$$

The operators $c_i^\dagger$ and c_i ($h_i^\dagger$ and h_i) create and annihilate an electron (a valence hole) in the single-particle state $|i\rangle$. The first and the second terms in Eq. (1) describe the kinetic energy of electrons and a valence hole in the dot, and the third and fourth terms describe the electron-electron and electron valence-hole scattering. Here $\langle ij|V|kl\rangle$ are the two-body matrix elements of the electron-electron[16] (ee) and electron valence-hole[13] (eh) Coulomb interactions, respectively.

The PL intensity $E(\omega)$ as a function of the photon frequency ω is given by the Fermi's golden rule:

$$E(\omega) = \sum_f |\langle \nu_f|\mathcal{P}|\nu_i\rangle|^2 \delta(\mathcal{E}^i - \mathcal{E}^f - \omega), \qquad (2)$$

where $|\nu_i\rangle$ and $|\nu_f\rangle$ are the initial and final states of the system, with corresponding energies $\mathcal{E}^i$ and $\mathcal{E}^f$ (we take $\hbar = 1$). The interband polarization operator $\mathcal{P} = \Sigma_{kl}\langle k|l\rangle c_k h_l$ removes an electron valence-hole pair from the ground state $|\nu_i\rangle$ of the photoexcited system. The selection rules are hidden in the electron-valence hole overlap matrix element $\langle k|l\rangle$. Since there is only a single valence hole we can define a purely electronic initial state $|\nu_i^k\rangle = \Sigma_l \langle k|l\rangle h_l |\nu_i\rangle$. The operator $\mathcal{P}$ creates a hole in the initial state: $\mathcal{P}|\nu_i\rangle = \Sigma_k c_k |\nu_i^k\rangle$, and the PL spectrum can be viewed as the spectral function of this hole.

A. Single-particle states

The single-particle electronic states $|k\rangle$ and the electron valence-hole pairs (excitons) in lens-shaped self-assembled quantum dots have been described in Ref. 12. The numerical calculations[12] show that the Fock-Darwin states are a good approximation to the single electron and single-hole states in a perpendicular magnetic field. The Fock-Darwin states $|nm,\sigma\rangle$ and energies $\varepsilon_{nm,\sigma} = \Omega_+(n+\frac{1}{2}) + \Omega_-(m+\frac{1}{2}) + g\mu_B \sigma B$ are those of a pair of harmonic oscillators. The last term is the Zeeman energy. The frequencies of the two oscillators are $\Omega_\pm = \frac{1}{2}(\Omega \pm \omega_c)$, where $\Omega^2 = \omega_0^2 + 4\omega_c^2$, $\omega_c = eB/m^*c$ is the cyclotron frequency, m^* is the effective mass, and ω_0 measures the effective confinement energy, appropriate to electrons or valence holes. The angular momentum for electrons is $R_e = m_e - n_e$, and for valence holes is $R_h = n_h - m_h$, opposite due to the opposite charge of a valence hole. An important property of the Fock-Darwin energy levels is that they form degenerate shells at the values of the magnetic field B for which $\Omega_+ = p\Omega_-$ with $p = 1, 2, \ldots$; at $B = 0$ (i.e., $p = 1$) we label these shells $s, p, d, f, \ldots$.

For typical 200 Å diameter InAs/GaAs dots the confining potentials are $\omega_{0e} = 50$ meV for electrons and $\omega_{0h} = 25$ meV for holes.[8,10] Up to five shells of bound electron and valence-hole levels were observed.[8,10] The difference between the electron and hole confinements partially compensates the effect of different effective masses, and the corresponding electron and hole Fock-Darwin orbitals overlap almost exactly.

The three characteristic energy scales appearing in the Hamiltonian (1): the kinetic energy (≈ 50 meV) greater than the Coulomb energy (≈ 30 meV) which is much greater than the Zeeman energy (≈ 0.1 meV/T) allow for a systematic perturbative calculation of energy levels.

B. Many-particle states

The interacting, initial many-particle states $|\nu_i\rangle$ are expanded in the basis of the noninteracting configurations of N electrons and a single valence hole: $|i_1, \ldots, i_N; j\rangle = c_{i_1}^\dagger \cdots c_{i_N}^\dagger h_j^\dagger |\text{vac}\rangle$, where $|\text{vac}\rangle$ stands for vacuum. The states are labeled by the total angular momentum R, the z component of the total spin of electrons S_z^i, and by the hole's spin σ_h, being good quantum numbers of the system. The valence hole mixes different electronic total angular momentum states. The Hamiltonian (1) is diagonalized numerically in each eigensubspace (R, S_z^i, σ_h).

We study the recombination from the lowest-energy state of the initial system. In this initial ground state the total spin of a partially filled shell ($=$ total electron spin S^i) is maximized in accordance with Hund's rule. The Hund's rule is verified numerically for up to the f shell, and used further for approximate calculations for larger numbers of electrons. Since for $S^i \neq 0$ the ground state is degenerate with respect to S_z^i, in the following we assume a weak magnetic field removing this degeneracy, and leading to a single lowest-energy configuration with a specified maximum S_z^i. The magnetic-field induced spin polarization of the partially filled shell will be shown to lead to a strong sensitivity of the PL spectrum to the polarization.

The final states of $N-1$ electrons $|\nu_f\rangle$, created by the annihilation of a single electron valence-hole pair in the state $|\nu_i\rangle$, are expanded in the basis of electron configurations $|i_1, \ldots, i_{N-1}\rangle = c_{i_1}^\dagger \cdots c_{i_{N-1}}^\dagger |\text{vac}\rangle$. The final states are also classified by their total angular momentum and spin (R, S_z^f).

C. Photoluminescence

The emission of light from the system of N electrons and a single valence-band hole is due to the annihilation of an electron valence-hole pair in the presence of $N-1$ excess electrons. The orbital selection rules are given by the overlap of electron and valence-hole Fock-Darwin orbitals $\langle n_e m_e | n_h m_h \rangle \approx \delta_{n_e n_h} \delta_{m_e m_h}$. The form of the interband polarization operator [cf. Eq. (2)] simplifies to $\mathcal{P} \sim \Sigma_i c_i h_i$. The operator $\mathcal{P}$ can be decomposed into a pair of operators with definite circular polarizations $\sigma_{+(-)}$: $\mathcal{P}_{+(-)} = \Sigma_{n_e m_e} \Sigma_{n_h m_h} \langle n_e m_e | n_h m_h \rangle c_{n_e m_e, \downarrow(\uparrow)} h_{n_h m_h, \uparrow(\downarrow)}$. The initial and final states connected by the operator $\mathcal{P}$ have the same angular momentum R, but the electron spin S_z differs by $\pm\frac{1}{2}$.

The recombination process is qualitatively illustrated in Fig. 1. Figure 1(a) shows an example of the initial configuration. The initial configuration corresponds to electrons and a valence hole filling up lowest kinetic energy single-particle states. For the valence hole this implies a lowest kinetic energy state $|00\rangle$ with two different spin configurations. The two different configurations correspond to different polarizations of emitted light. Because the valence hole relaxed to the top of the valence band, the removal of an electron valence-hole pair $\mathcal{P}_{+(-)}|\nu_i\rangle \approx c_{00,\downarrow(\uparrow)} h_{00,\uparrow(\downarrow)} |\nu_i\rangle$ creates a hole (vacancy) in the $|00\rangle$ state of the electron system, as illustrated in Fig. 1(b). The photoluminescence spectrum corresponds to a spectral function of this hole.

A vacancy in the $|00\rangle$ state corresponds to an excited state of the electron system. This excited state may be degenerate with a number of other configurations, some of them illustrated in Figs. 1(c) and 1(d). The degeneracies of the initial and final-state configurations give rise to a complex recombination spectrum, which depends on the number of electrons N.

III. RESULTS AND DISCUSSION

We describe here the results of the numerical calculation of the emission spectrum. The initial ground state $|\nu_i\rangle$ and all
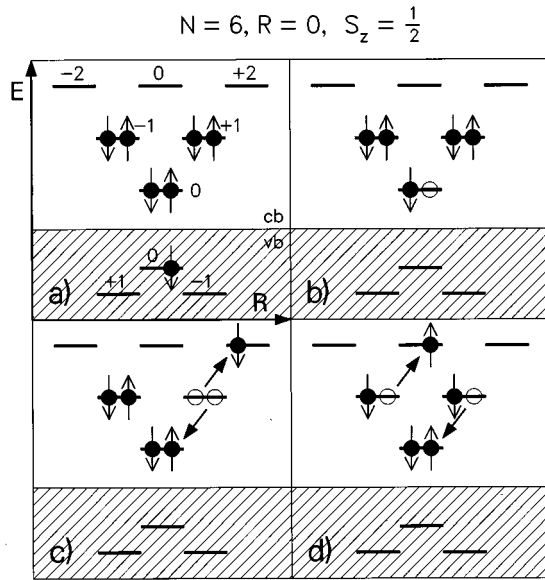
N = 6, R = 0, $S_z = \frac{1}{2}$

FIG. 1. Energy as a function of angular momentum of electronic configurations for $N=6$: (a) initial ground state; (b)–(d) degenerate final states. Open circles indicate holes in shells s and p.

final eigenstates $|\nu_f\rangle$ are obtained through the numerical diagonalization of the initial and final Hamiltonians for up to $N=9$ electrons. The many-particle states were built from up to 15 Fock-Darwin states corresponding to five shells. The initial and final Hilbert spaces were limited to all lowest kinetic energy configurations corresponding to degenerate shells plus all excited configurations with the kinetic energy not exceeding $4\omega_{0e}$. The convergence of calculations was guaranteed by the strong quantization of the single-particle energies in the dot, described, e.g., by the ratio of the characteristic Coulomb energy to the electron intershell spacing $\langle V \rangle/\omega_{0e} < \langle 00,00|V_{ee}|00,00\rangle/\omega_{0e} = 0.6$.

A. Polarization σ_-

The evolution of the total angular momentum R and the total spin of electrons S^i of the initial state $|\nu_i\rangle$, as a function of N, is shown at the bottom of Fig. 2. The oscillations of the total angular momentum and total spin correspond to the filling up of electronic shells. The total spin of filled shells is zero, but half-filled shells are spin polarized, in agreement with Hund's rule. We will show that the maximum-spin configuration of partially filled shells has a strong effect on the recombination spectrum.

In the top frame of Fig. 2 we show the numerically calculated emission spectra (full circles) for polarization σ_- as a function of N. This polarization corresponds to the removal of a spin-up electron and an increase of the total electronic spin $S^f = S_z^f = S^i + \frac{1}{2}$. The area of the circles is proportional to the intensity of individual transitions. The empty circles correspond to an approximate calculation. There are two features of the evolution of the emission spectrum with N: (a) the appearance of plateaus at $N=2-4$ and $N=6-9$, and (b) the splitting of the emission line for $N>4$.

The plateaus can be explained within the single-configuration approximation (SCA) (empty circles). The SCA corresponds to the emission from the lowest kinetic
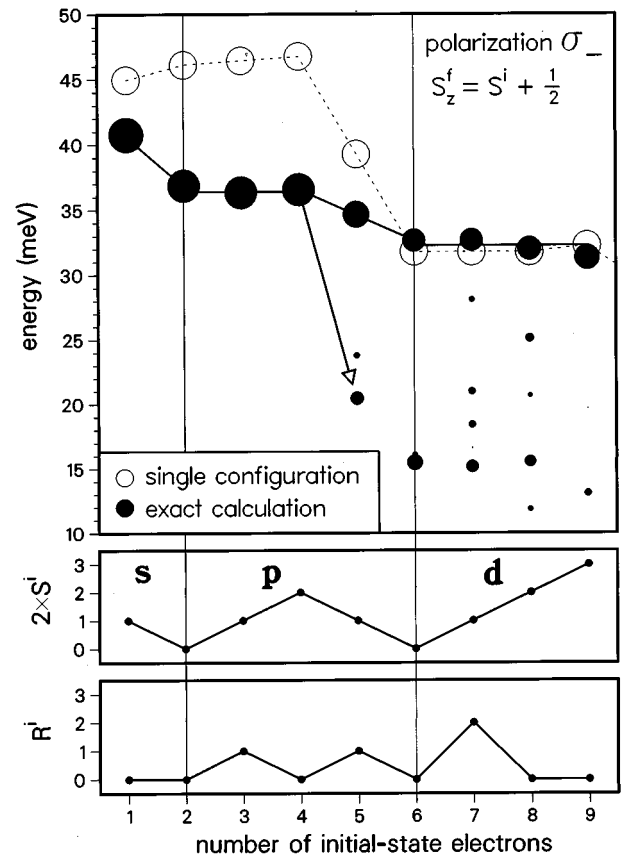
FIG. 2. Emission spectrum for the σ_- polarization as a function of number of electrons N. Areas of circles are proportional to intensities of individual transitions. Full circles—exact diagonalization, empty circles—single-configuration approximation. The arrow shows a splitting of the main peak. Bottom frames: total spin of electrons S^i and total angular momentum R in the initial state; filled shells are indicated.

energy configuration consistent with Hund's rule. The emission energy ω has three components: (i) kinetic energy of the annihilated electron valence-hole pair, (ii) electron valence-hole pair attraction, and (iii) the interaction of this pair with the excess $N-1$ electrons. In the SCA the first two components are independent of N. Due to charge neutrality of the electron valence-hole complex, the third component is mainly due to exchange. It depends strongly on the spin of electrons in the partially filled shell. Until the shell is half-filled, consecutive electrons are added with spin down, increasing the total spin of this shell (equal to the total spin S^i). There is no exchange interaction between the spin-polarized shell and the removed s-shell spin-up electron and we observe a plateau. After the half filling is reached, electrons are added with spin up (decreasing S^i) and can exchange with the removed s-shell spin-up electron. The removed electron's energy decreases with increasing number of same-spin electrons, until the shell is filled and the next plateau begins. This effect survives including mixing between configurations, and even though the steps separating plateaus shrink significantly, it should be observable as a reflection of the shell structure of a quantum dot.

The second effect is the splitting of the emission spectrum. As indicated in Fig. 2 with an arrow, the splitting ap-

pears for $N \gtrsim 5$. The splitting is due to many degenerate configurations in the final state. Some of them are shown in Fig. 1. Due to Coulomb interactions these Auger-like configurations (c,d) are mixed with the optical configuration (b), created by $\mathcal{P}$ acting on the initial configuration (a), and contribute to the recombination spectrum.

B. Polarization σ_+

Let us now turn to the σ_+ polarization. In this polarization a spin-down electron is removed, and the projection of the total electronic spin is reduced: $S_z^f = S^i - \frac{1}{2}$. Unlike for σ_-, the final-state configuration $\mathcal{P}_+|\nu_i\rangle$ is not an eigenstate of the total spin S^f and has finite projections on a pair of subspaces: $S^f = S^i + \frac{1}{2}$ and $S^f = S^i - \frac{1}{2}$. The σ_+ emission spectrum splits therefore into a pair of subspectra: $E(\omega) = \alpha_+ E_+(\omega) + \alpha_- E_-(\omega)$, corresponding to the final states from the two S^f subspaces. The subspectra are weighted by the overlaps of the spin functions: $\alpha_\pm = |\langle \nu^f | \mathcal{T}_{S^i \pm 1/2} | \nu^f \rangle|^2$, where the operator $\mathcal{T}_S$ projects onto spin S. The subspectrum E_+ repeats the σ_- spectrum (but with a reduced intensity), and the subspectrum E_- appears only in this (σ_+) polarization.

The photoluminescence spectrum measured at any polarization is a combination of the two subspectra, with E_+ appearing in the σ_- channel, and both E_+ and E_- in the σ_+ channel. If $S^i = 0$ (closed shells in the initial state), i.e., for $N = 2,6,12,20, \ldots$, E_+ and E_- are identical and the photoluminescence spectrum is insensitive to the polarization. However, the polarization of the spectrum strongly depends on the polarization of the spin $S^i \neq 0$.

The emission spectrum for polarization σ_+ is shown in Fig. 3. The two components E_+ and E_- are marked with full and empty circles, respectively. The inset shows results in SCA for a larger number of electrons. The E_+ spectrum has been discussed already. There are two different features appearing in the E_- spectrum: (a) the emergence of the lower-energy line at $N = 3$, and (b) the emergence of the higher-energy line at $N = 9$. The emergence of the lower-energy line for $N > 2$ is related to the spin configuration of the partially filled shell. The removed electron in the s shell has its spin parallel to the spin of electrons in the partially filled shell, and therefore the energy difference is proportional to the energy of exchange interaction between these two shells (s and p for $N = 3$).

The emergence of the higher-energy line at $N = 9$ is a very different effect. The recombination spectrum shown up to $N = 8$ always involved excited final states, with a hole (vacancy) in the zero angular momentum state $|00\rangle$ of the s shell. When the d shell begins to fill, a second zero angular momentum state $|11\rangle$ becomes available. Hence, a lower-energy state of the final configuration, with the hole relaxed from the s shell to the d shell, becomes optically active due to the mixing via the Coulomb interactions. The position of the new line is governed by the large kinetic energy of a corresponding single electron excitation ($\sim 2\omega_{0e} = 100$ meV).

Figure 3 collects all the features in the photoluminescence spectrum, appearing with increasing number of electrons N (charging of the dot), discussed throughout this section: (i) band-gap renormalization and the plateaus in the main line;
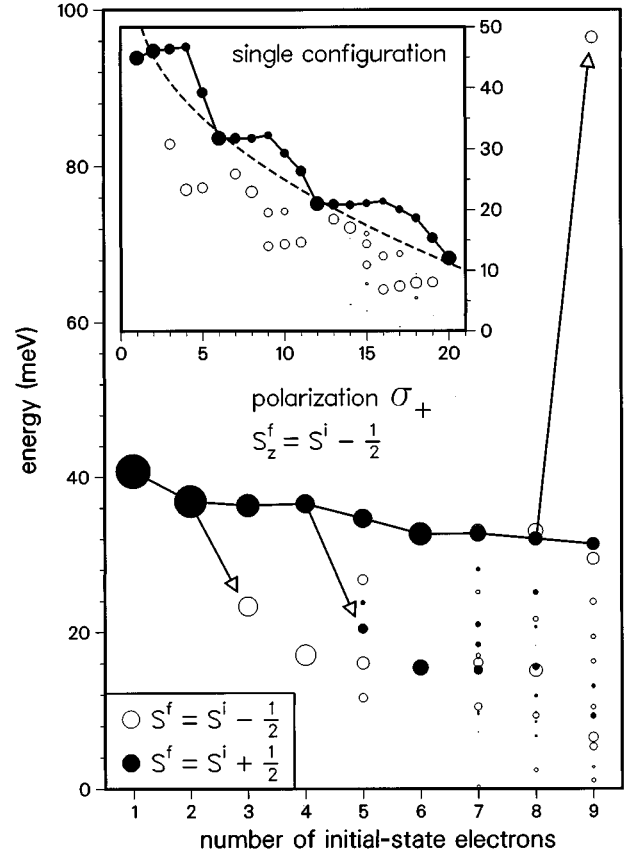

FIG. 3. Emission spectrum for the σ_+ polarization as a function of number of electrons N. Areas of circles are proportional to intensities of individual transitions. The spectrum has been resolved into two total-spin subspaces (full and empty circles). Arrows show splittings of the main peak. Inset: single-configuration approximation.

(ii) splitting of the recombination line toward lower energy for $N > 2$, proportional to intershell exchange energy; (iii) splitting of the main line toward lower energy at $N > 4$, due to mixing of a number of degenerate configurations; and (iv) splitting of the emission line toward higher energy at $N = 9$, due to coupling with the ground state of the final system.

C. Band-gap renormalization

We now turn to the problem of the redshift of the emission line with an increasing number of electrons N, i.e., the band-gap renormalization. Having verified through numerical diagonalization that the SCA describes fairly well the energy of the emission line, we can use the SCA to extend the calculations to large N.

In the inset to Fig. 3 we show the results for $N = 1-20$, i.e., for up to four electronic shells completely filled in the initial state. The full circles show the position of the main emission peak, i.e., the subtraction energy of an s-shell exciton. For closed valence shells in the initial state ($N = 2,6,12,20, \ldots$) these energies fall on the dashed (square-root) curve. The curve corresponds to the exchange interaction of a $k = 0$ electron in a two-dimensional electron gas: $\int d^2k V_{ee}(k) n(k) \sim \sqrt{N}$. Due to a large gap in the single-
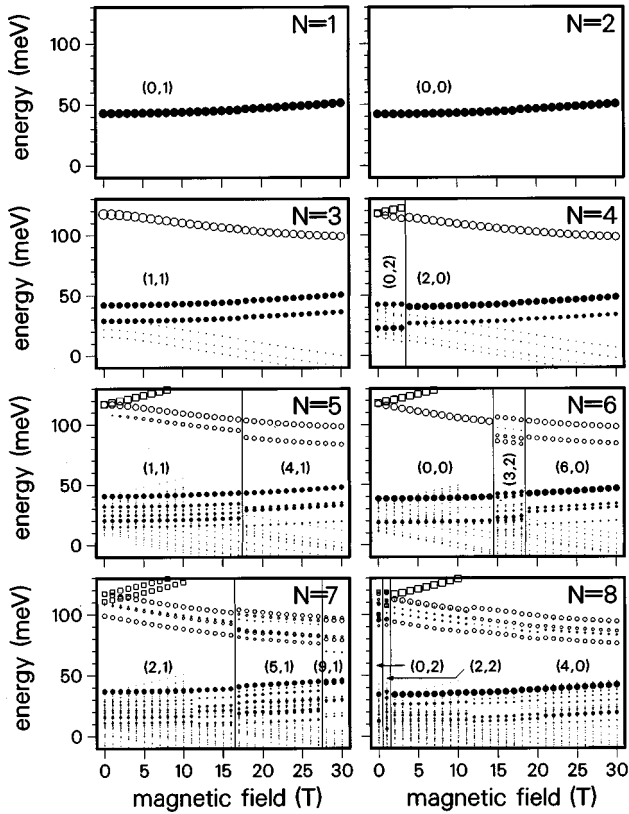
FIG. 4. Magnetic-field evolution of the emission spectra for $N=1-8$ electrons in the initial state. Areas of symbols are proportional to intensities of individual transitions. Vertical lines show transitions in the ground state of initial systems, with the total spin of electrons and total angular momentum indicated as $(R, 2 \times S^i)$. Full circles—ground state recombination, empty circles and squares—valence-band hole trapped in the p shell.

particle spectrum, the bare exchange energy of filled shells appears to well describe the band-gap renormalization as a function of the number of electrons N. However, for partially filled shells the renormalization is modified by correlation energy. The correlation effect is largest for the maximum valence-shell spin S^i, which coincides with the half filling of this shell ($N=4,9,16, \dots$).

D. Effects of magnetic field and temperature

The magnetic field removes degeneracies of electronic shells and induces crossing of Fock-Darwin levels. The removal of the shell degeneracies destroys the maximum-spin configurations within the partially filled shells. We will concentrate on the emission in the σ_+ polarization channel; the σ_- polarization, requiring a population of spin-flipped holes, occurs only at a finite temperature.

The calculated emission spectra for $N=1-8$ and $B=0-30$ T are shown in Fig. 4. The full circles show emission from the ground state with (R, S^i) as the initial ground state configurations and with the vertical lines showing the corresponding intervals of B. One can follow the smooth evolution of the spectrum with increasing field and the effects of the field-induced transitions in the initial state, described in detail for the system of electrons in Ref. 11. The open symbols show emission from excited states, with elec-
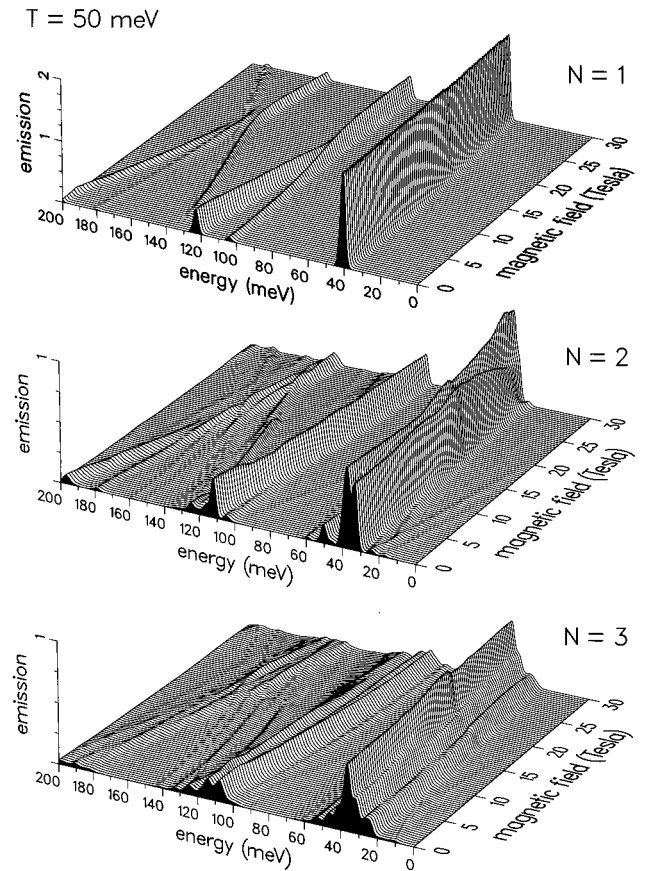

FIG. 5. Magnetic-field evolution of the emission spectra for $N=1-3$ electrons in the initial state assuming Boltzmann distribution of initial states with an effective temperature $T=\omega_{0e}=50$ meV.

trons relaxed to their lowest-energy configuration, but the valence hole trapped in either of the $|01\rangle$ and $|10\rangle$ states of the p shell. The nonequilibrium population of valence holes would allow for a direct recombination with the equilibrium electrons.

The exact calculation of the photoluminescence from excited initial states requires a knowledge of the complicated relaxation processes in the system. Assuming a quasi-equilibrium reached during cw excitation, the initial states are populated according to the Boltzmann distribution with an effective temperature T. The quasiequilibrium emission spectrum is then given by $E(T,\omega) \sim \Sigma_i e^{-\mathcal{E}^i/T} E^i(\omega)$, where the summations are over all possible initial eigenstates of the system, including all possible spin and angular momentum subspaces. The magnetic-field evolution of such spectra calculated for $N=1-3$ and $T=\omega_e=50$ meV are shown in Fig. 5. In order to account for a large number of closely spaced transitions, discrete peaks have been broadened with Gaussians with the width of 2 meV.

The main difference between the three spectra in Fig. 5 is, apart from the discussed earlier band-gap renormalization, significant broadening of peaks with increasing N due to a rapidly increasing number of optical transitions from excited initial states. For $N=2$ a new peak ($\omega=33.2$ meV at $B=0$) emerges below the main line ($\omega=37.5$ meV at $B=0$). The peak corresponds to the recombination from an

excited state with an electron and a valence hole in the *s* shell and one extra electron in the *p* shell. The total spin of electrons is $S^i = 1$, and therefore the transition energy is lowered by the exchange interaction. For $N = 3$ the broadening destroys the simple structure of a pair of peaks at $T = 0$, shown in Fig. 4.

IV. CONCLUSION

Using exact diagonalization techniques we have studied numerically the photoluminescence spectrum from a modulation-doped self-assembled quantum dot as a function of the number of electrons N. The total spin and total angular momentum of the ground state of an exciton and excess electrons oscillate as a function of the number of electrons, with the total spin reaching a maximum for partially occupied electronic shells. The photoluminescence spectrum has been related to the spectral function of the hole (vacancy) created in this correlated electron ground state. We have shown that there are oscillations and splittings of the photoluminescence spectra, which can be directly related to the number of electrons in the dot and to electron-electron interactions. The dependence of the band-gap renormalization on the number of carriers has been determined. We have studied the evolution of the emission spectra with the magnetic field and the effect of the nonequilibrium population of valence-band holes. The polarization of calculated spectra is very sensitive to the spin polarization of electronic configurations in the dot. It is hoped that this work will stimulate future experiments.

*Permanent address: Institute of Physics, Technical University of Wrocław, Wybrzeże Wyspiańskiego 27, 50-370 Wrocław, Poland.

[1] For a recent review, see P. M. Petroff and S. P. Denbaars, Superlatt. Microstruct. **15**, 15 (1994).

[2] N. Kirstaedter, N. N. Ledentsov, M. Grundmann, D. Bimberg, V. M. Ustinov, S. S. Ruvimov, M. V. Maximov, P. S. Kop'ev, Zh. I. Alferov, U. Richter, P. Werner, U. Gösele, and J. Heydenreich, Electron. Lett. **30**, 1416 (1994); M. Grundmann, J. Christen, N. N. Ledentsov, J. Bohrer, D. Bimberg, S. S. Ruvimov, P. Werner, U. Richter, U. Gosele, J. Heydenreich, V. M. Ustinov, A. Yu. Egorov, A. E. Zhukov, P. S. Kop'ev, and Zh. I. Alferov, Phys. Rev. Lett. **74**, 4043 (1995).

[3] J.-Y. Marzin, J.-M. Gérard, A. Izraël, D. Barrier, and G. Bastard, Phys. Rev. Lett. **73**, 716 (1994).

[4] R. Notzel, J. Temmyo, and T. Tamamura, Nature (London) **369**, 131 (1994).

[5] S. Fafard, R. Leon, D. Leonard, J. L. Merz, and P. M. Petroff, Phys. Rev. B **52**, 5752 (1995).

[6] H. Drexler, D. Leonard, W. Hansen, J. P. Kotthaus, and P. M. Petroff, Phys. Rev. Lett. **73**, 2252 (1994).

[7] S. Raymond, S. Fafard, P. J. Poole, A. Wojs, P. Hawrylak, S. Charbonneau, D. Leonard, R. Leon, P. M. Petroff, and J. L. Merz, Phys. Rev. B **54**, 11 548 (1996).

[8] K. H. Schmidt, G. Medeiros-Ribeiro, M. Oestreich, P. M. Petroff, and G. H. Döhler, Phys. Rev. B **54**, 11 346 (1996).

[9] H. Lipsanen, M. Sopanen, and J. Ahopelto, Phys. Rev. B **51**, 13 868 (1995).

[10] M. Fricke, A. Lorke, J. P. Kotthaus, G. Medeiros-Ribeiro, and P. M. Petroff, Europhys. Lett. **36**, 197 (1996).

[11] A. Wojs and P. Hawrylak, Phys. Rev. B **53**, 10 841 (1996); P. Hawrylak, Phys. Rev. Lett. **71**, 3347 (1993).

[12] A. Wojs, P. Hawrylak, S. Fafard, and L. Jacak, Phys. Rev. B **54**, 5604 (1996).

[13] A. Wojs and P. Hawrylak, Phys. Rev. B **51**, 10 880 (1995).

[14] P. Hawrylak, A. Wojs, and J. A. Brum, Solid State Commun. **98**, 847 (1996); Phys. Rev. B **54**, 11 397 (1996).

[15] A. Wojs and P. Hawrylak, Solid State Commun. **100**, 487 (1996).

[16] P. Hawrylak, Solid State Commun. **88**, 475 (1993).